

Unparticle Physics in di-photon production at the LHC

M. C. Kumar^{a,b *}, Prakash Mathews^{a †}, V. Ravindran^{c ‡}, Anurag Tripathi^{c §}

a) Saha Institute of Nuclear Physics, 1/AF Bidhan Nagar, Kolkata 700 064, India.

b) School of Physics, University of Hyderabad, Hyderabad 500 046, India.

*c) Regional Centre for Accelerator-based Particle Physics,
Harish-Chandra Research Institute, Chhatnag Road, Jhansi, Allahabad, India.*

ABSTRACT

We have considered the diphoton production in the unparticle physics at the LHC. The contributions of spin-0 and spin-2 unparticles to the di-photon production are studied in the invariant mass and other kinematical distributions, along with their dependencies on the model dependent parameters. It is found that the signal corresponding to the unparticles is significant for moderate values of the couplings.

*mc.kumar@saha.ac.in

†prakash.mathews@saha.ac.in

‡ravindra@mri.ernet.in

§anurag@mri.ernet.in

1 Introduction

Banks and Zaks [1] studied gauge theories with non-integral number, N_F , of Dirac fermions, such that the two loop beta function vanishes. At this nontrivial infra-red (IR) fixed point, the theory is scale invariant and does not have a particle interpretation. Motivated by Banks and Zaks, Georgi [2] proposed the following scheme: Theory at very high energy contains the fields of the standard model (SM) and fields of a sector called Banks-Zaks \mathcal{BZ} sector, with a nontrivial IR fixed point. These two sectors interact through exchange of particles with a large mass scale $M_{\mathcal{U}}$. Below $M_{\mathcal{U}}$ the couplings have generic form

$$\frac{1}{M_{\mathcal{U}}^k} O_{\text{SM}} O_{\mathcal{BZ}} , \quad (1)$$

where O_{SM} and $O_{\mathcal{BZ}}$ are operators built out of the standard model and the \mathcal{BZ} fields respectively. Scale invariance in the \mathcal{BZ} sector emerges at energy scale $\Lambda_{\mathcal{U}}$. In the effective theory below $\Lambda_{\mathcal{U}}$ the interaction of (1) matches onto

$$C_{\mathcal{U}} \frac{\Lambda_{\mathcal{U}}^{d_{\mathcal{BZ}} - d_{\mathcal{U}}}}{M_{\mathcal{U}}^k} O_{\text{SM}} O_{\mathcal{U}} , \quad (2)$$

where $d_{\mathcal{U}}$ is the scaling dimension of unparticle operator $O_{\mathcal{U}}$. $M_{\mathcal{U}}$ should be large enough that its coupling to SM be sufficiently weak. Few of the generic operators that can describe the interaction of unparticle fields with those of the SM are found to be

$$\frac{\lambda_s}{\Lambda_{\mathcal{U}}^{d_{\mathcal{U}}}} T_{\mu}^{\mu} O_{\mathcal{U}}, \quad \frac{\lambda_v}{\Lambda_{\mathcal{U}}^{d_{\mathcal{U}}-1}} \bar{\psi} \gamma_{\mu} \psi O_{\mathcal{U}}^{\mu}, \quad \frac{\lambda_t}{\Lambda_{\mathcal{U}}^{d_{\mathcal{U}}}} T_{\mu\nu} O_{\mathcal{U}}^{\mu\nu} . \quad (3)$$

The dimensionless coupling λ_{κ} corresponds to the unparticle operator $O_{\mathcal{U}}^{\kappa}$, where $\kappa = s, v, t$ refers to the scalar, vector and tensor operators respectively. $T_{\mu\nu}$ is the energy momentum tensor of the SM. These operators are Hermitian and transverse.

The unparticle propagator [3] is given by

$$\int d^4x e^{iPx} \langle 0 | T O_{\mathcal{U}}^{\kappa}(x) O_{\mathcal{U}}^{\kappa}(0) | 0 \rangle = \frac{i A_{d_{\mathcal{U}}}}{2 \sin(d_{\mathcal{U}} \pi)} \frac{B_{\kappa}}{(-P^2 - i\epsilon)^{2-d_{\mathcal{U}}}} , \quad (4)$$

where, B_{κ} depends on the Lorentz structure of the operator $O_{\mathcal{U}}$ as given below:

$$\begin{array}{ll}
O_{\mathcal{U}} & 1 \\
O_{\mathcal{U}}^{\rho} & \eta_{\mu\nu}(P) = -g_{\mu\nu} + \frac{P_{\mu}P_{\nu}}{P^2} \\
O_{\mathcal{U}}^{\rho\sigma} & B_{\mu\nu\alpha\beta}(P) = \frac{1}{2} (\eta_{\mu\alpha}\eta_{\nu\beta} + \eta_{\mu\beta}\eta_{\nu\alpha} - \frac{2}{3}\eta_{\mu\nu}\eta_{\alpha\beta}) \quad .
\end{array}$$

The constant $A_{d_{\mathcal{U}}}$ is given by

$$A_{d_{\mathcal{U}}} = \frac{16\pi^{5/2}}{(2\pi)^{2d_{\mathcal{U}}}} \frac{\Gamma(d_{\mathcal{U}} + 1/2)}{\Gamma(d_{\mathcal{U}} - 1)\Gamma(2d_{\mathcal{U}})} \quad . \quad (5)$$

where $1 < d_{\mathcal{U}} < 2$.

If $\Lambda_{\mathcal{U}}$ is of order TeV, unparticle dynamics can be seen at the Large Hadron Collider (LHC) through various high energy scattering processes and hence the phenomenology with it will be interesting. Several detailed studies on the phenomenology of unparticle physics have been reported in the recent past exploring the possibility of explaining the known experimental results and also constraining the parameters of the model. Supersymmetric scenarios were taken up in [4] and effects on cosmology and astrophysics have been considered in [5]. For studies in flavor physics and CP violations, see [6]. In the context of neutrino physics, the unparticle physics has been studied by authors of [7]. Study of [8] showed that unparticles can be represented as an infinite tower of massive particles with controllable mass-squared spacing Δ^2 , and that pure unparticles cannot decay, while for small Δ the decay is possible. In [9], lowest order ungravity correction to the Newtonian gravitational potential has been computed and it is found that $1 < d_{\mathcal{U}} < 2$ leads to modification of the inverse square law with r dependence in the range $1/r^2$ and $1/r^4$ and also explored on how to discriminate extra dimension models and ungravity models in sub milli-meter tests of gravity. It was found in [10] that the unparticles can modify the coupling between Higgs and a pair of gluons/photons and its effects can be observed in di-photon productions through Higgs decay processes at the LHC. Unparticle contributions to mono-jet, and di-photon production at e^+e^- colliders are now known [11].

Drell-Yan production at hadron collider via unparticles has been reported in [12], where we had restricted ourselves to scalar and tensor unparticles to find out the plausible

region of the parameter space to see their effect. We had also incorporated next to leading order QCD effects to stabilise our results against both higher order corrections and scale variations. We list in [13] most of the articles in the context of unparticle physics. In this paper, we have studied the impact of unparticle fields on one of the important processes, namely di-photon production.

2 The Diphoton production

The production of di-photon system is one of the important processes at the hadron colliders and has been used to do precision study of the Standard Model (SM). Also it provides a laboratory for probing new physics. In the SM, this process has been studied in great detail including higher order QCD [14] effects. The soft gluon effects through threshold resummation have also been incorporated (see [15]). In the context of physics beyond the SM, this process has played an important role in constraining parameters of various models. For example, models with large extra dimensions can be probed using the di-photon signals [16] (See also [17] for the bounds coming from the Tevatron). In this paper, we study the effect of unparticles on various kinematical distributions of di-photon system produced at hadron colliders. At hadron colliders, the di-photon system can be produced through

$$P_1(p_1) + P_2(p_2) \rightarrow \gamma(p_3) + \gamma(p_4) + X(p_X) , \quad (6)$$

where P_i are the incoming hadrons with momenta p_i and X is the final inclusive hadronic state. The hadronic cross sections can be obtained by convoluting the partonic cross sections $d\hat{\sigma}^{ab}$ with the appropriate incoming parton distribution functions f_a^P :

$$d\sigma(P_1 P_2 \rightarrow \gamma \gamma X) = \sum_{a,b=q,\bar{q},g} \int f_a^{P_1}(x_1) f_b^{P_2}(x_2) d\hat{\sigma}^{ab}(x_1, x_2) dx_1 dx_2 . \quad (7)$$

Here, x_1 and x_2 are the momentum fractions of the incoming partons in the hadrons P_1 and P_2 respectively.

The unparticle model has spin-0 and spin-2 unparticles. Thus, di-photon can be produced through $q\bar{q}$ annihilation as well as the gg fusion subprocesses with scalar and tensor unparticles appearing as propagators (see Eq.(4)). These partonic sub-processes occur at leading order in couplings λ_s and λ_t . At this order spin-1 unparticle does not contribute.

The matrix element squared of the partonic subprocess due to scalar unparticle is found to be

$$\begin{aligned} |\overline{M}_{q\bar{q}}|^2 &= \frac{1}{8N_c} \lambda_s^4 \chi_{\mathcal{U}}^2 \left(\frac{s}{\Lambda_{\mathcal{U}}^2} \right)^{2d_{\mathcal{U}}-1}, \\ |\overline{M}_{gg}|^2 &= \frac{1}{8(N_c^2-1)} \frac{1}{4} \lambda_s^4 \chi_{\mathcal{U}}^2 \left(\frac{s}{\Lambda_{\mathcal{U}}^2} \right)^{2d_{\mathcal{U}}}. \end{aligned} \quad (8)$$

Similarly, we have for tensor unparticle exchange:

$$\begin{aligned} |\overline{M}_{q\bar{q}}|^2 &= \frac{1}{8N_c} \left[e^4 Q_f^4 8 \left(\frac{u}{t} + \frac{t}{u} \right) \right. \\ &\quad \left. - 8e^2 Q_f^2 \lambda_t^2 \chi_{\mathcal{U}} \cos(d_{\mathcal{U}}\pi) \left(\frac{s}{\Lambda_{\mathcal{U}}^2} \right)^{d_{\mathcal{U}}} \frac{1}{s^2} (u^2 + t^2) \right. \\ &\quad \left. + 2 \lambda_t^4 \chi_{\mathcal{U}}^2 \left(\frac{s}{\Lambda_{\mathcal{U}}^2} \right)^{2d_{\mathcal{U}}} \frac{1}{s^4} t u (u^2 + t^2) \right], \\ |\overline{M}_{gg}|^2 &= \frac{1}{8(N_c^2-1)} 2 \lambda_t^4 \chi_{\mathcal{U}}^2 \left(\frac{s}{\Lambda_{\mathcal{U}}^2} \right)^{2d_{\mathcal{U}}} \frac{1}{s^4} (u^4 + t^4). \end{aligned} \quad (9)$$

where, Q_f is the electric charge of the parton of flavour f , $\chi_{\mathcal{U}} = A_{d_{\mathcal{U}}}/(2 \sin(d_{\mathcal{U}}\pi))$ and N_c is the number of colors. The variables s, t and u are the standard partonic Mandelstam invariants. Notice that only tensor unparticles interfere with the SM subprocess amplitudes. In the above matrix elements (Eqs. (8,9)), we have already done spin and colour averages and included the correct symmetry factor coming from the identical nature of the final state photons. It may be noted here that the spin-0 and spin-2 unparticles do not interfere.

As was pointed out in [18], the $gg \rightarrow \gamma\gamma$ box contribution at order α_s^2 could give a sizeable effect at the LHC in comparison to other contributions to this order due

to large gluon flux. There are numerous diagrams that contribute to order α_s^2 , but the authors of [18] have argued that the dominant contribution comes from the box diagram. For unparticle searches it is plausible that the interference of the gg unparticle contributions with the SM diagrams at order α_s^2 could be sizeable. In the context of large extra-dimensional models, these interference contributions enhance the effect at small Q regions [16]. For our present analysis we have restricted to only the LO in QCD.

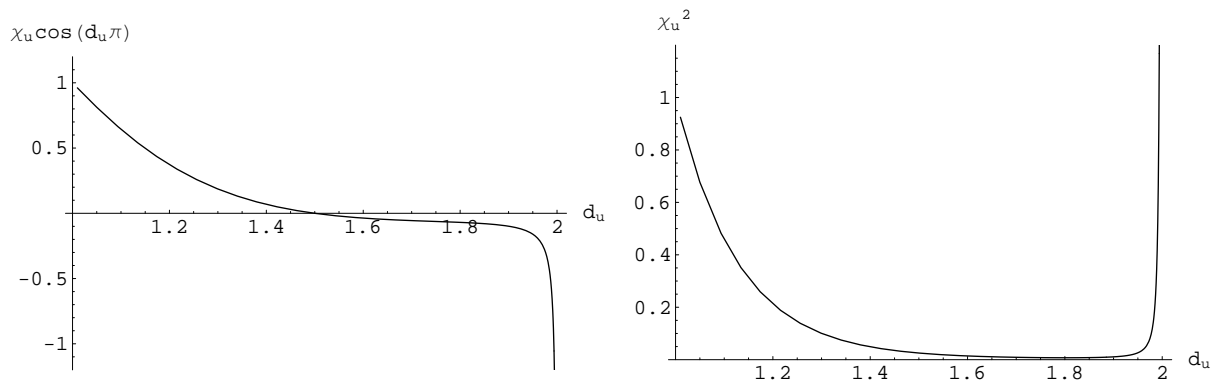


Figure 1: The function $\chi_u \cos(\pi d_u)$ (left) and χ_u^2 (right) showing its variation with the scaling dimension d_u of the unparticle operator.

Unitarity imposes constraint [19] on the conformal dimension \P of these operators, which for scalar unparticle is $d_u > 1$. Though this constraint restricts the scalar unparticle sector, for our numerical analysis we have considered $d_u > 1$ as the general constraint for other unparticle operators (say tensor unparticle) as well. Before, we present the effects of unparticles on various distributions of di-photon system at the LHC, we discuss the coefficients $\chi_u \cos(d_u \pi)$ and χ_u^2 that enter the interference and direct unparticle contributions respectively. In Fig. (1), we have plotted them against the scaling dimension d_u of the unparticle operator. χ_u is negative when $1 < d_u < 2$ and singular as $d_u \rightarrow 2$. As $d_u \rightarrow 1$, χ_u approaches a limiting value, here both χ_u^2 and $\chi_u \cos(d_u \pi)$ are positive and large and as we go below $d_u = 1.01$, the variation is found to be mild. In the plateau

^{\P}There exist no known examples of scale invariant local field theories that are not conformally invariant (Y. Nakayama in [4]).

region, where $1.3 < d_{\mathcal{U}} < 1.9$, these functions are almost constant and relatively small. We avoid the region $1.9 \leq d_{\mathcal{U}} \leq 2.0$ where $\chi_{\mathcal{U}}$ is very rapidly increasing. Hence, in this region, the unparticle effects can not be probed. With this information, the value of $d_{\mathcal{U}}$ is chosen in such a way that the unparticle effects can be seen at the LHC energy.

The couplings of the unparticle operators to the SM fields are given by

$$\lambda_{\kappa} = C_{\mathcal{U}}^{\kappa} \left(\frac{\Lambda_{\mathcal{U}}}{M_{\mathcal{U}}} \right)^{d_{\mathcal{BZ}}} \frac{1}{M_{\mathcal{U}}^{d_{\text{SM}}-4}}, \quad (10)$$

A priori we have no information on any of the parameters in the above equation. For our numerical analysis we have taken λ_{κ} in the range $0.4 \leq \lambda_{\kappa} < 1$, so that the unparticle effects are treated as perturbation. The other parameter that appears in this model is $\Lambda_{\mathcal{U}}$ which we choose to be 1 TeV.

In the following, we will study the effects of scalar and tensor unparticles separately. We will analyse these effects only for the LHC with $\sqrt{S} = 14$ TeV. A similar analysis for the Tevatron can be done with our numerical code that incorporates all the analytical results presented in this paper. We have considered four different distributions of the photons in the final state to unravel the effects coming from the unparticles. They are (a) invariant mass distribution $d\sigma/dQ$, where Q is the invariant mass of the di-photon system, (b) angular distribution $d\sigma/d\cos\theta^*$, (c) the rapidity (Y) distributions of the di-photon system and (d) rapidity (y^{γ}) distributions of the individual photons. We have imposed the cuts: rapidity $|y^{\gamma}| < 2.5$, and transverse momentum of the photons $p_T^{\gamma} > 40$ GeV [20] for all the distributions that we have reported here in order to make our predictions for an environment which is as close as possible to that of the experiment. Moreover, for the invariant mass distribution, in order to suppress the SM background and also to enhance the signal we have imposed an angular cut on the photons $|\cos\theta_{\gamma}| < 0.8$, where θ_{γ} is the angle of the photons in the lab frame. Similarly, for the angular and rapidity distributions, to suppress the background, we have considered only those events that satisfy the constraint $Q > 600$ GeV. For all our plots, we have used MRST 2001 leading order (LO) parton density sets [21].

2.1 Invariant mass distribution

In this section, the invariant mass distribution $d\sigma/dQ$ is studied, where $Q^2 = (p_3 + p_4)^2$. In Fig.2 we have plotted this distribution including the effects of scalar (left panel) and tensor (right panel) unparticles for Q between $100 < Q < 900$ GeV. Here we have chosen $d_{\mathcal{U}} = 1.01$ and $\Lambda_{\mathcal{U}} = 1$ TeV. With this choice of parameters, we find that the unparticle effects can be seen only in the large Q region. In addition, we have presented different contributions coming from various sub-processes to the cross section for both spin-0 and spin-2 unparticles to see their effects separately. In the spin-0 case, the quark anti-quark initiated process dominates over the gluon initiated process due to higher power of scale in the later case. On the other hand, we see the opposite behavior for the spin-2 case. In the spin-2 case, this behavior can be understood by noticing that the gluon fluxes are much larger compared to quark anti-quark fluxes at the LHC energies even though the couplings (λ_{κ}) for both quark anti-quark (pure unparticle contribution) and gluon initiated processes are same. In addition, the interference term, being negative reduces the contribution coming from quark anti-quark channel. Notice that there is no such contribution from the spin-0 unparticle.

In Fig.3, we show the variation of the invariant mass distribution with respect to the scaling dimension $d_{\mathcal{U}}$ of the scalar and tensor unparticle operators, for $\Lambda_{\mathcal{U}} = 1$ TeV. As expected, we find that the unparticle effects show up significantly when the value of $d_{\mathcal{U}}$ decreases. When $d_{\mathcal{U}}$ is around 1.9, the unparticle effects are completely washed away. The interference term in the spin-2 unparticle case gives large negative contribution only in the region where $d_{\mathcal{U}}$ is less than 1.3 (see Fig. 1).

We have also studied the effects of λ_t and λ_s variations on the distributions. They are shown in Fig. 4 for $d_{\mathcal{U}} = 1.01$. From Fig. 3 and Fig. 4, we see that in the region where $d_{\mathcal{U}}$ is below 1.1 and λ_s above 0.6 the scalar unparticle contribution is substantial even at low energies.

The invariant mass distribution for a higher value of the scale $\Lambda_{\mathcal{U}} = 2$ TeV is plotted

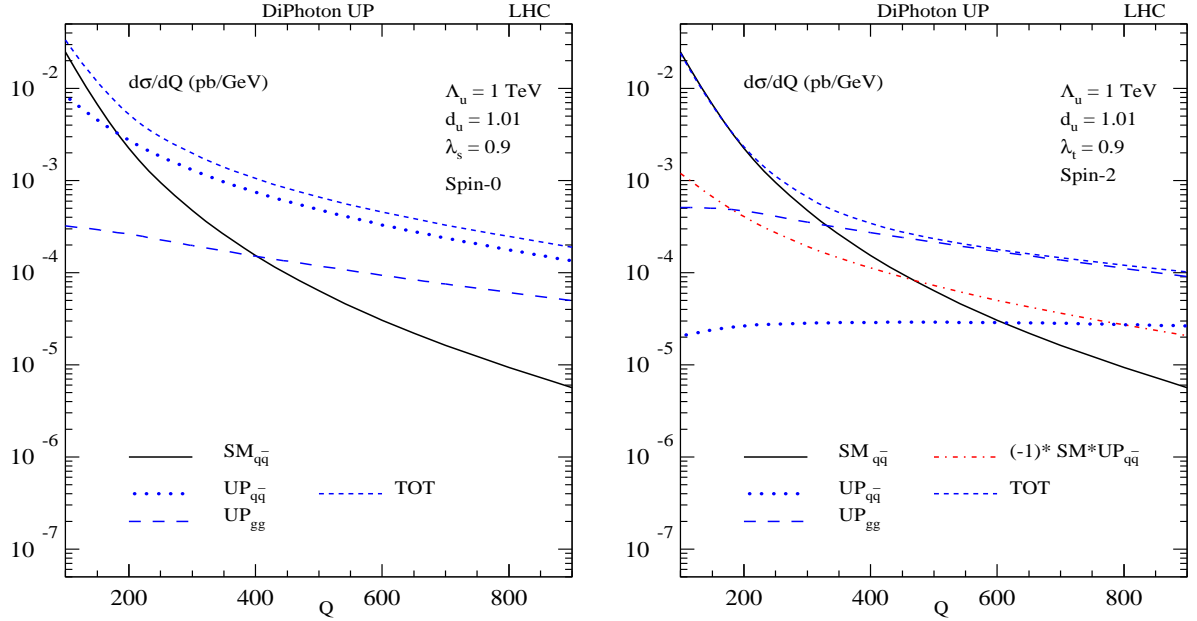


Figure 2: The contribution of the various sub processes to the di-photon production in the invariant mass distribution via scalar (left) and tensor (right) s -channel processes, with $d_U = 1.01$ and $\Lambda_U = 1$ TeV. The scalar and tensor couplings are taken to be $\lambda_{s,t} = 0.9$. We imposed an angular cut $|\cos \theta_\gamma| < 0.8$ on the photons to suppress the SM background.

in Fig. 5 for various values of λ_κ and d_U . Due to the factor $\Lambda_U^{-d_U}$ in Eqs.(8,9) the cross sections are suppressed as we increase Λ_U . In the rest of the paper, we choose $\lambda_s = 0.6$, $\lambda_t = 0.9$, $d_U = 1.01$ for $\Lambda_U = 1$ TeV to study other distributions.

2.2 Angular distribution

The angular distribution $d\sigma/d\cos \theta^*$ is studied in the center of mass frame of the final state photons. The angle θ^* is defined by

$$\cos \theta^* = \frac{p_1 \cdot (p_3 - p_4)}{p_1 \cdot (p_3 + p_4)}, \quad (11)$$

where p_3 and p_4 are the final state photon momenta. The distributions are plotted in the range $-0.95 < \cos \theta^* < 0.95$ for both spin-2 and spin-0 cases. We take $d_U = 1.01$, $\Lambda_U = 1$ TeV, $\lambda_t = 0.9, 0.4$ and $\lambda_s = 0.6, 0.4$. This angular distribution is computed in the

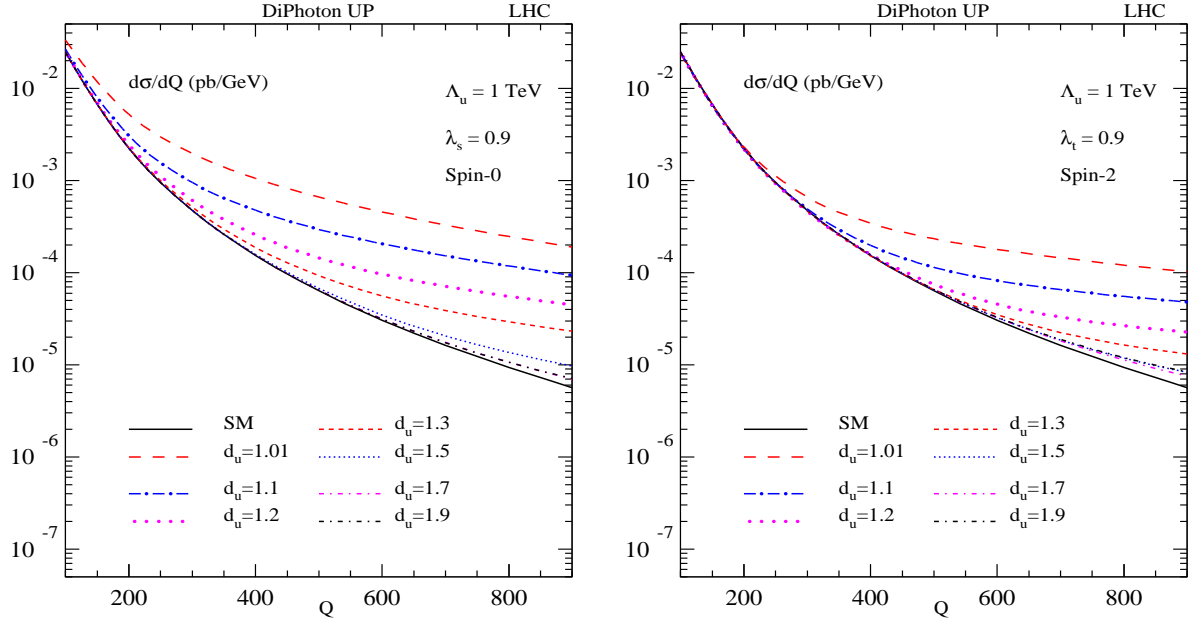


Figure 3: Invariant mass distribution plotted for different values of d_u for spin-0 (left) and spin-2 (right) with $\Lambda_u = 1$ TeV and $\lambda_s, \lambda_t = 0.9$, with an angular cut on the photons $|\cos \theta_\gamma| < 0.8$.

region where Q between 600 GeV and $0.9\Lambda_u$ contributes. In this region, the unparticle effects are expected to be large.

The angular distributions for both spin-2 and spin-0 are given in Fig. 6. These distributions for spin-2 and spin-0 differ both in magnitude and in structure. For spin-2 case with $\lambda_t = 0.9$, we find that the unparticle effects show up significantly. While for $\lambda_t = 0.4$, the negative interference term dominates over the pure unparticle contribution bringing down the distributions. On the other hand, the scalar unparticle contribution for this choice of parameters is significant for both $\lambda_s = 0.4, 0.6$.

2.3 Rapidity

In this section, we consider the rapidity distributions of the di-photon system ($d\sigma/dY$) as well as of individual final state photons ($d\sigma/dy^\gamma$). Rapidity of the di-photon system

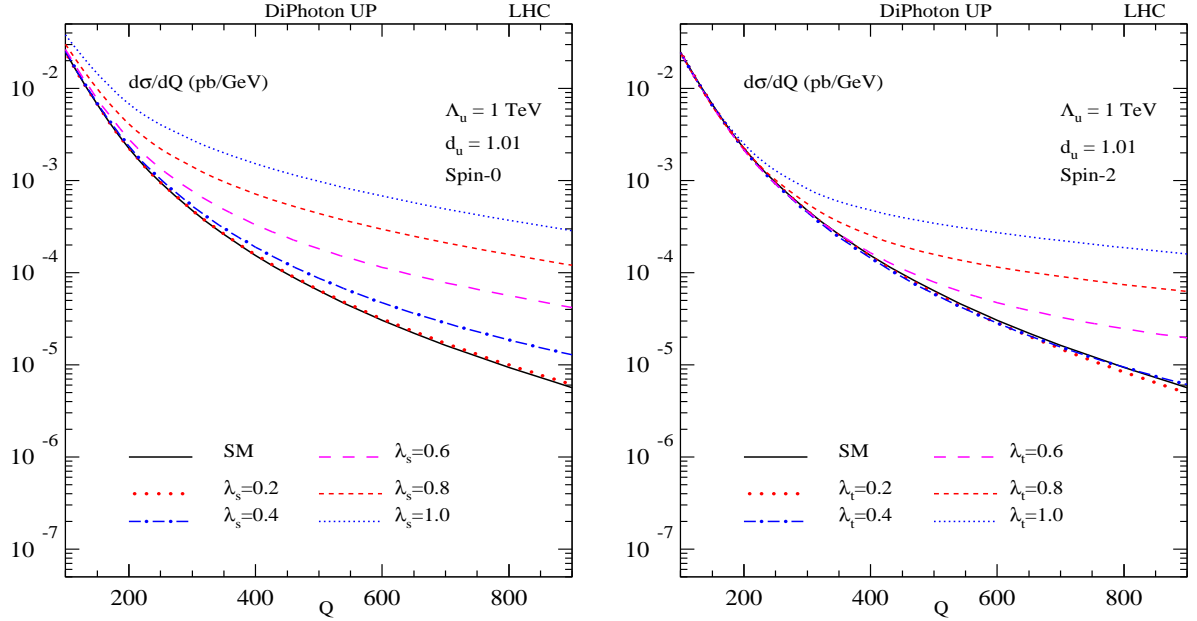


Figure 4: Invariant mass distribution is plotted for various values of the coupling λ_s and λ_t for spin-0 (left) and spin-2 (right) respectively with $\Lambda_{\mathcal{U}} = 1$ TeV and $d_{\mathcal{U}} = 1.01$, with an angular cut on the photons $|\cos \theta_\gamma| < 0.8$.

is defined as

$$Y = \frac{1}{2} \log \left(\frac{p_2 \cdot q}{p_1 \cdot q} \right), \quad (12)$$

here $q = p_3 + p_4$. For the rapidity distributions of the individual photons, we have to replace q in the above equation by their momenta.

We have presented the rapidity distributions of di-photon system for both SM + scalar unparticle and SM + tensor unparticle in Fig. 7. We have chosen $d_{\mathcal{U}} = 1.01$ and $\Lambda_{\mathcal{U}} = 1$ TeV. We find that the deviation from the SM is large in the central region ($Y=0$). For the spin-0 case and for both the choices $\lambda_s = 0.6$ and 0.4 , the unparticle effect is quiet large whereas for the spin-2 case, this is true only for larger λ_t .

We have presented the rapidity of the individual final state photons including the unparticle contributions in Fig. 8 for $d_{\mathcal{U}} = 1.01$ and $\Lambda_{\mathcal{U}} = 1$ TeV. The scalar unparticle contribution with $\lambda_s = 0.6$ is again large in the central region whereas for the tensor

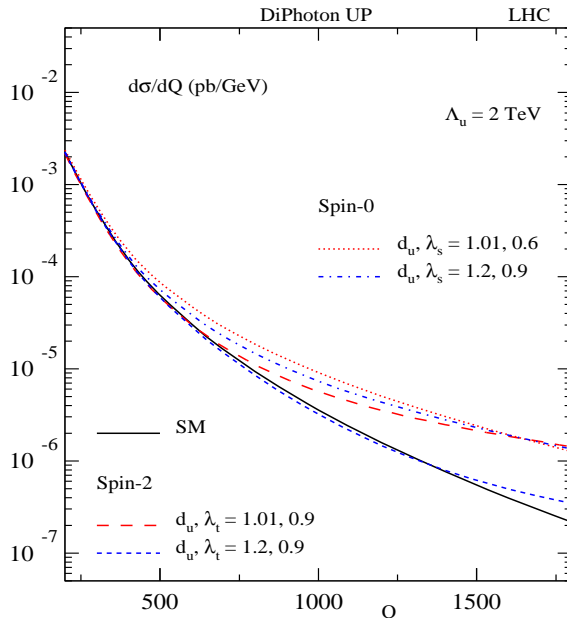


Figure 5: Invariant mass distribution $d\sigma/dQ$ for the di-photon production with $\lambda_s = 0.6$ and $\lambda_t = 0.9$ for $\Lambda_U = 2$ TeV for both $d_U = 1.01$ and 1.2 . We have imposed an angular cut $|\cos \theta_\gamma| < 0.8$ on the photons.

unparticle case to see the larger effect λ_t has to be closer to 1. For smaller values of $\lambda_{s,t}$, that is below 0.4, the effects are unnoticeable.

3 Conclusions

In this paper we have studied the effects of scalar and tensor unparticles on the di-photon production at the LHC. Various kinematical distributions are analysed to see their effects. The spin-0 and spin-2 unparticle effects could be clearly distinguishable from SM background differing by around an order of magnitude in most of the distributions that we have considered. We have essentially three unknown parameters in this model, namely the scale Λ_U , the scaling dimension d_U and the coupling λ_κ . The impact of these parameters on these distributions is studied in detail. We find that the effects of scalar unparticle (Fig. 4) with the coupling λ_s closer to 1 emerge even at lower energies.

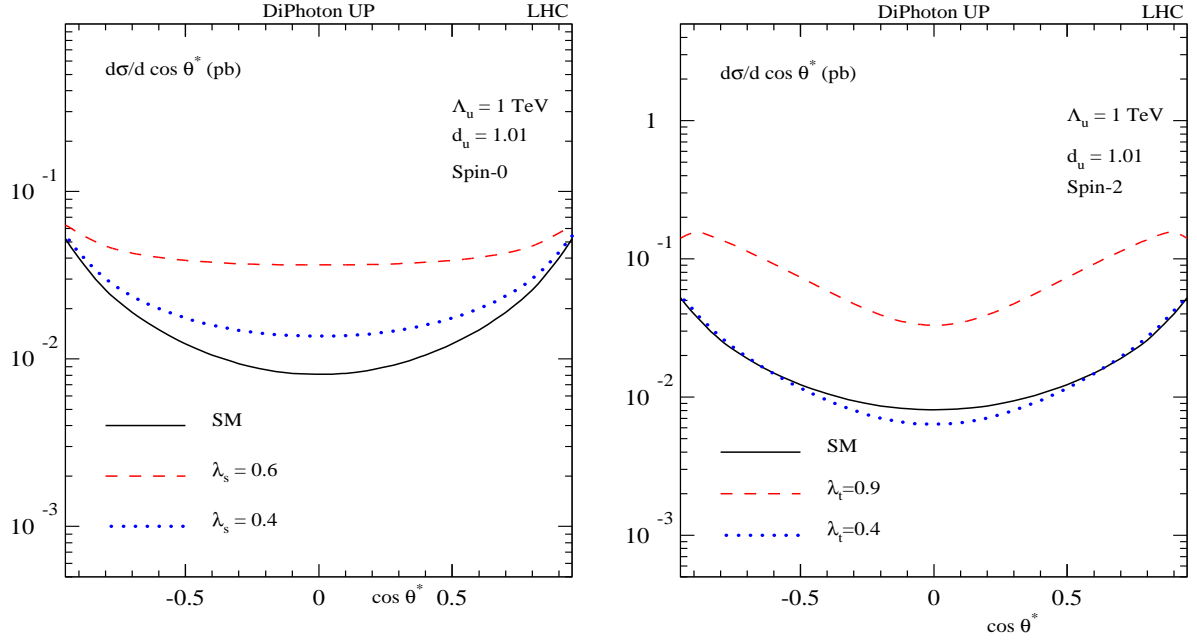


Figure 6: Angular distributions $d\sigma/d\cos\theta^*$ of the photons for spin-0 (left) and spin-2 (right) with $\Lambda_{\mathcal{U}} = 1$ TeV and $d_{\mathcal{U}} = 1.01$. We have taken couplings $\lambda_s = 0.6, 0.4$ and $\lambda_t = 0.9, 0.4$ integrating Q in the range $600 \text{ GeV} < Q < 0.9\Lambda_{\mathcal{U}}$.

We have chosen λ_s below 0.6 for $d_{\mathcal{U}} = 1.01$ and $\Lambda_{\mathcal{U}} = 1$ TeV for our analysis. In case, the nature has both scalar and tensor unparticles, our results can give cross sections without any further work as these two do not interfere. We conclude by noting that the di-photon production can be used to unravel various effects coming from this new model with unparticles.

Acknowledgments:

M.C.Kumar (SRF) would like to thank CSIR, New Delhi, India for the financial support. Anurag would like to thank Theory Division, SINP, Kolkata for the hospitality where a part of this work was done. PM would like to thank the Abdus Salam ICTP for hospitality under the Associates program, when this work was being completed.

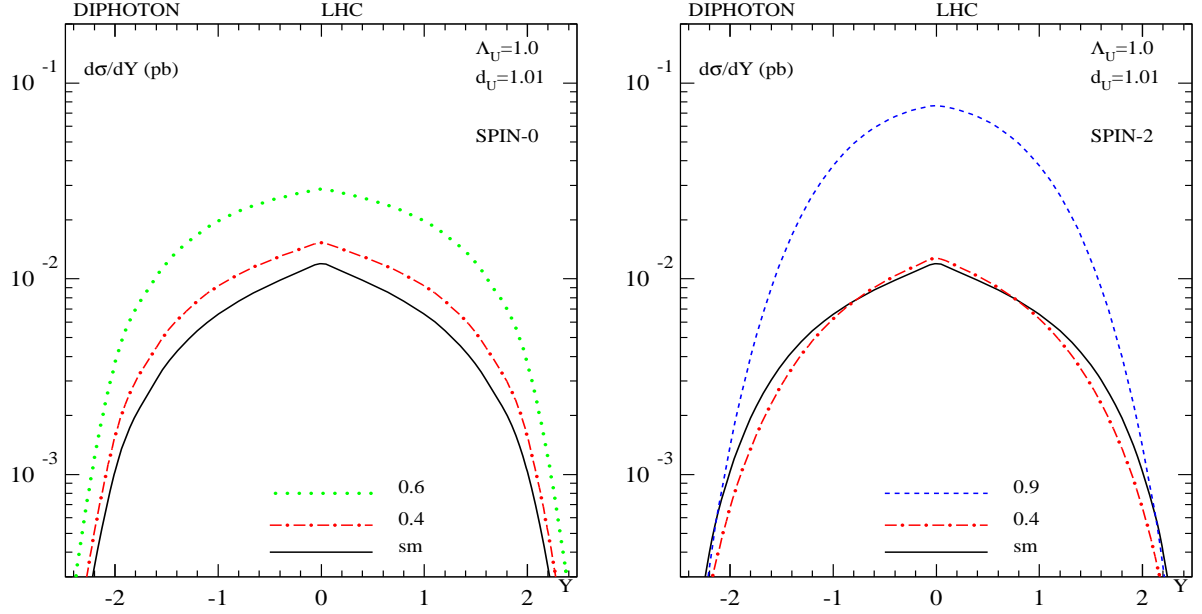


Figure 7: Rapidity distributions $d\sigma/dY$ of the di-photon system for spin-0 (left) and spin-2 (right) with $\Lambda_U = 1$ TeV and $d_U = 1.01$. We have taken the couplings to be $\lambda_s = 0.6, 0.4$ and $\lambda_t = 0.9, 0.4$ with Q in the region $600 \text{ GeV} < Q < 0.9\Lambda_U$.

References

- [1] T. Banks and A. Zaks, Nucl. Phys. B **196**, (1982) 189.
- [2] H. Georgi, Phys. Rev. Lett. **98**, (2007) 221601, arXiv:hep-ph/0703260.
- [3] H. Georgi, Phys. Lett. B **650**, (2007) 275, arXiv:0704.2457 [hep-ph]; K. Cheung, W. Y. Keung and T. C. Yuan, arXiv:0704.2588 [hep-ph].
- [4] P. J. Fox, A. Rajaraman and Y. Shirman, arXiv:0705.3092 [hep-ph]; H. Zhang, C. S. Li, Z. Li, arXiv:0707.2132 [hep-ph]; Y. Nakayama, arXiv:0707.2451 [hep-ph]; N. G. Deshpande, X. G. He, J. Jiang, arXiv:0707.2959 [hep-ph]; T. A. Ryttov, F. Sannino, arXiv:0707.3166 [hep-ph].
- [5] H. Davoudiasl, arXiv:0705.3636 [hep-ph]; S. Hannestad, G. Raffelt, Y. Y. Y. Wong, arXiv:0708.1404 [hep-ph], A. Freitas and D. Wyler, arXiv:0708.4339 [hep-ph].

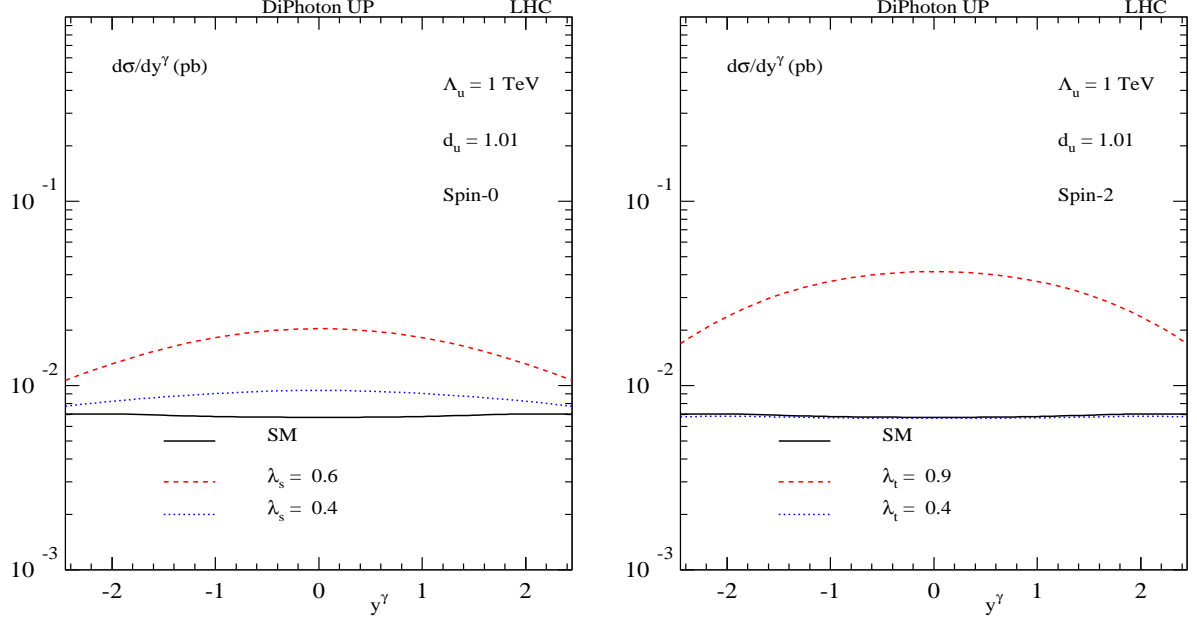


Figure 8: Rapidity distributions $d\sigma/dy^\gamma$ of the photons for spin-0 (left) and spin-2 (right) with $\Lambda_u = 1$ TeV and $d_u = 1.01$. We have taken the couplings to be $\lambda_s = 0.6, 0.4$ and $\lambda_t = 0.9, 0.4$, with Q in the range $600\text{GeV} < Q < 0.9\Lambda_u$.

- [6] C. H. Chen and C. Q. Geng, arXiv:0705.0689 [hep-ph]; G. J. Ding and M. L. Yan, arXiv:0705.0794 [hep-ph]; T. M. Aliev, A. S. Cornell and N. Gaur, arXiv:0705.1326 [hep-ph]; X. Q. Li and Z. T. Wei, Phys. Lett. B **651** (2007) 380-383 arXiv:0705.1821 [hep-ph]; C. D. Lu, W. Wang and Y. M. Wang, arXiv:0705.2909 [hep-ph]; T. M. Aliev, A. S. Cornell and N. Gaur, JHEP 0707:072,2007, arXiv:0705.4542 [hep-ph]; C. H. Chen, C. Q. Geng, arXiv:0706.0850 [hep-ph]; Roman Zwicky, arXiv: 0707.0677; R. Mohanta, A. K. Giri, arXiv:0707.1234 [hep-ph]; C. S. Huang, X. H. Wu, arXiv:0707.1268 [hep-ph]; A. Lenz, arXiv:0707.1535 [hep-ph]; R. Mohanta, A.K.Giri, arXiv:0707.3308 [hep-ph]. C. H. Chen and C. Q. Geng, arXiv:0709.0235 [hep-ph].

- [7] S. Zhou arXiv:0706.0302 [hep-ph]; X. Q. Li, Y. Li, Z. T. Wei, arXiv:0707.2285 [hep-ph]; D. Majumdar, arXiv:0708.3485 [hep-ph], L. Anchordoqui and H. Goldberg,

arXiv:0709.0678 [hep-ph].

- [8] M. A. Stephanov, arXiv:0705.3049 [hep-ph].
- [9] H. Goldberg, P. Nath, arXiv:0706.3898 [hep-ph]
- [10] T. Kikuchi, N. Okada, arXiv:0707.0893 [hep-ph].
- [11] K. Cheung, W. Keung, T. Yuan, arXiv:0706.3155 [hep-ph]
- [12] Prakash Mathews, V. Ravindran, Phys.Lett.**B657**:198-206,2007, arXiv:0705.4599 [hep-ph]
- [13] M. Luo and G. Zhu, arXiv:0704.3532 [hep-ph]; Y. Liao, arXiv:0705.0837 [hep-ph]; N. Greiner, arXiv:0705.3518 [hep-ph]; D. Choudhury, D. K. Ghosh, Mamta, arXiv:0705.3637 [hep-ph]; Shao-Long Chen, Xiao-Gang He, arXiv:0705.3946 [hep-ph]; G. J. Ding, M. L. Yan, arXiv:0706.0325 [hep-ph]; Y. Liao, J. Y. Liu, arXiv:0706.1284 [hep-ph]; M. Bander, J. L. Feng, A. Rajaraman, Y. Shriman, arXiv:0706.2677 [hep-ph]; T. G. Rizzo, arXiv: 0706.3025 [hep-ph]; S. L. Chen, X. G. He and H. C. Tsai, arXiv:0707.0187 [hep-ph]; J. J. Bij, S. Dilcher, arXiv:0707.1817 [hep-ph]; D. Choudhury, D. K. Ghosh, arXiv:0707.2074 [hep-ph]; A. Delgado, J. R. Espinosa, M. Quiros, arXiv:0707.4309 [hep-ph]; G. Cacciapaglia, G. Marandella, J. Terning, arXiv:0708.0005 [hep-ph]; M. Neubert, arXiv:0708.0036 [hep-ph]; M. X. Luo, W. Wu, G. H. Zhu arXiv:0708.0671 [hep-ph]. N. G. Deshpande, S. D. H. Hsu, J. Jiang arXiv:0708.2735 [hep-ph]; G. Bhattacharyya, D. Choudhury, D. K. Ghosh, arXiv: 0708.2835 [hep-ph]; Yi Liao, arXiv:0708.3327 [hep-ph]; A. T. Alan, N. K. Pak, arXiv:0708.3802; T. i. Hur, P. Ko and X. H. Wu, arXiv:0709.0629 [hep-ph]. I. Gogoladze, N. Okada and Q. Shafi, arXiv:0708.4405 [hep-ph].
- [14] T. Binoth, J. P. Guillet, E. Pilon and M. Werlen, Eur. Phys. J. C **16** (2000) 311 [arXiv:hep-ph/9911340].

- [15] C. Balazs, E. L. Berger, P. M. Nadolsky, C. P. Yuan Phys. Rev. D76:013009, 2007
- [16] O. J. P. Eboli, T. Han, M. B. Magro and P. G. Mercadante Phys. Rev. D61:094007, 2000; K. Cheung, Greg L. Landsberg Phys. Rev D62 (2000) 076003
- [17] CDF Collaboration, PRL 95, 091801 (2005); arXiv:0707.2294 [hep-ex]
- [18] Z. Bern, L. Dixon, C. Schmidt, Phys.Rev. D66:074018, 2002; hep-ph/0206194
- [19] G. Mack Commun. Math. Phys. 55, 1
- [20] CMS Collaboration Physics Technical Design Report, J. Phys. G: Nucl. Part. Phys. 34 995-1579.
- [21] A. D. Martin, R. G. Roberts, W. J. Stirling and R. S. Thorne, Phys. Lett. B **531** (2002) 216 [arXiv:hep-ph/0201127].